INNOVATION

Imaging the coordination of multiple signalling activities in living cells

Christopher M. Welch, Hunter Elliott, Gaudenz Danuser and Klaus M. Hahn

Abstract | Cellular signal transduction occurs in complex and redundant interaction networks, which are best understood by simultaneously monitoring the activation dynamics of multiple components. Recent advances in biosensor technology have made it possible to visualize and quantify the activation of multiple network nodes in the same living cell. The precision and scope of this approach has been greatly extended by novel computational approaches (referred to as computational multiplexing) that can reveal relationships between network nodes imaged in separate cells.

Methods such as phosphoproteomics[1], protein–protein interaction studies[2] and gene expression profiling[3] allow the analysis of signalling networks via the simultaneous observation of every pathway component. However, these methods average information over many cells and do not take into account cell-to-cell heterogeneity, which has been shown to play key parts in the function of signalling networks[4–6]. Flow cytometry allows the measurement of signalling at the single cell level[7] but, similar to proteomic methods, temporal information is available only as an average across many cells, and spatial information is either completely absent or available only at very coarse levels, such as compartmentalization in organelles or at the plasma membrane.

A 'tool chest' of fluorescent proteins emitting light from the ultraviolet (UV) to the near-infrared parts of the spectrum has made it possible to simultaneously visualize the subcellular dynamics of multiple proteins in the same living cell — a technique that is referred to as experimental multiplexing. Such multiplexed imaging, which can reveal the coordination of two or more subcellular structures, is now routinely exploited to study, for example, the interactions of cytoskeletal fibres[8,9], the transient coupling of adhesion molecules and cytoskeleton flows[10], and the choreography of protein recruitment to endocytic sites at the plasma membrane[11]. By contrast, the subcellular coordination of the signalling events that regulate these dynamics has remained considerably more obscure. In some cases, a single signalling activity can be visualized together with the dynamics of subcellular structures. However, until recently, this has been restricted largely to second messengers, for example, using fluorescent chelators that report ion concentrations[12,13], or fluorescently tagged domains that bind accumulations of lipid second messengers[14,15] or mark cellular structures[16]. The study of the coordinated activation of multiple signalling proteins has been hindered by formidable technical hurdles. These obstacles have been recently overcome by two very different but complementary approaches — the development of powerful new biosensors and the development of computational multiplexing.

> "These experimental multiplexing approaches may ultimately enable us to visualize the activities of three or more signalling molecules at the same time."

To understand the spatiotemporal dynamics of signalling events, it is generally not sufficient to simply follow the changing localization of proteins. Signalling proteins interact with downstream targets only in specific activated states. Therefore, to dissect the mechanism of signal transduction, it is necessary to monitor both protein localization and activation. Biosensors have been devised to report protein activation states, usually relying on fluorescence resonance energy transfer (FRET) readouts of a conformational change or protein interaction[17,18]. Owing to the availability of fluorescent proteins spanning much of the visible spectrum, FRET-based biosensors can now be built using fluorescent proteins with orthogonal wavelengths, enabling the imaging of two biosensors in the same cell. Furthermore, a deeper understanding of fluorescent proteins has permitted the design of biosensors that respond directly to endogenous signalling molecules, without the need to use two fluorescent proteins. These experimental multiplexing approaches may ultimately enable us to visualize the activities of three or more signalling molecules at the same time.

However, even with these improved designs, only a limited number of biosensors can be introduced into one cell. In addition, multispectral imaging and the introduction of multiple exogenous proteins are often accompanied by increased phototoxicity and the perturbation of cell physiology. Ideally, one could study the dynamics of each protein species separately, in different cells, and subsequently relate the data to each other via correlation with a fiduciary event that is common to each cell. Indeed, this approach has been applied to study the timing of signalling events during phagocytosis and wound closure[19–21]. However, many cellular functions display stochastic behaviours, resulting in a wide range of heterogeneous signalling patterns. In this case, establishing the relationships between signalling activities that are not all observed in the same cell is more challenging.

Recent work by several laboratories has begun to break through this barrier. It has been shown that spatiotemporal relationships between any two cellular activities observed together can be extracted from their constitutive, basal fluctuations[22–24]. It has also been shown that, when measuring the relationships between two pairs of activities in different cells, with one activity in

common between the pairs, it is possible to predict the spatiotemporal relationships among all three individual activities, even when they are observed in different cells[22]. This process has been referred to as computational multiplexing in order to distinguish it from experimental multiplexing. Although computational multiplexing is still in its very early days, it may ultimately become the technology of choice for reconstructing complex pathways with many component activities. Importantly, the concept of computational multiplexing relies on concurrent measurements of activities in pairs, triplets or even quadruplets. The more relationships that can be extracted through direct observation in single experiments, the more robust the computationally inferred relationships between signalling components will be. Therefore, advances in experimental multiplexing will lay the groundwork for advances in computational multiplexing.

The goal of this Innovation article is to outline the current state of both experimental and computational multiplexing, and to project their joint potential for the analysis of signal transduction at the single cell level.

Experimental multiplexing

The great majority of experiments studying multiple signalling nodes in the same living cell have been accomplished by combining genetically encoded FRET biosensors, the most tractable and commonly used type of biosensor. These have been extended to multiplexing primarily through the development of new FRET pairs with orthogonal wavelengths and advances in instrumentation and techniques that enhance sensitivity. Both of these developments are important, as the primary limitation to experimental multiplexing appears to be the ability of living cells to tolerate multiple exogenous reporter molecules. A host of other developing approaches show promise, some of which require the use of only one fluorophore to monitor each activity, and some of which cause significantly reduced cell perturbation.

Multiplexing with genetically encoded FRET. Although several different FRET pairs have been used to construct biosensors (for example, blue fluorescent protein (BFP) and cyan fluorescent protein (CFP), enhanced green fluorescent protein (EGFP) and *Discosoma* spp. red fluorescent protein (DsRed), and CFP and yellow fluorescent protein (YFP)), the CFP and YFP pair has to date proven to be the most useful in multiplexing, owing to its superior fluorescence properties and its excitation and emission wavelengths, which are compatible with other fluorophores. The development of orange and red proteins that are spectrally distinct from CFP and YFP[25] and the subsequent improvement in their photostability and brightness[26,27] have provided compatible FRET pairs for multiplexing (see Supplementary information S1 (figure) and Supplementary information S2 (table)). In an impressive example of multiparameter imaging, Piljic and Schultz[28] studied two, three and four activities simultaneously (FIG. 1a). These authors used two CFP and YFP FRET probes (a cytoplasmic calcium- and calmodulin-dependent kinase IIα (CaMKIIα) sensor and a membrane-bound protein kinase C (PKC) sensor), together with an orthogonal monomeric Orange (mOrange) and mCherry FRET pair in a sensor for the assembly of annexin 4 (a calcium-dependent phospholipid-binding protein). This enabled spatially resolved, ratiometric imaging using FRET. By restricting themselves to monitoring only the FRET intensity changes of the annexin 4 biosensor, the authors were able to follow the kinetics of annexin assembly into a trimer, which is facilitated by calcium influx, together with changes in calcium levels (observed by monitoring Fura Red). These two activities could then be correlated with the activities of CaMKIIα and PKC signalling in live cells to determine the time sequence of calcium influx, cellular signalling and the resultant annexin 4 assembly.

> “advances in experimental multiplexing will lay the groundwork for advances in computational multiplexing.”

Rather than use FRET pairs that are compatible with CFP and YFP, Ai *et al.*[29] generated new fluorophores and combined mTeal and mCitrine with mAmetrine and tandem dimeric Tomato (tdTomato) to image nucleus-targeted and nucleus-excluded caspase 3 activity within the same cell (FIG. 1b). mAmetrine is a unique fluorophore with a large Stokes shift and a violet-shifted excitation spectrum; this allows its effective separation from mTeal. The T-Sapphire and DsRed combination has also been used in combination with a CFP and YFP FRET pair, to detect cyclic GMP concentrations[30]. But, as T-Sapphire has an excitation spectrum that is similar to CFP, and a large Stokes shift that allows FRET to be performed with DsRed, this fluorophore permits simultaneous excitation of two spectrally separable FRET pairs. Recently, ‘ultramarine’ fluorophores, with excitation or emission wavelengths in the violet range of the spectrum, have emerged[31,32]. These require cell irradiation with more ‘toxic’ UV light but may enable simultaneous imaging of three FRET biosensors when paired with another violet-shifted fluorophore, such as BFP.

Imaging fluorescence lifetime rather than fluorescence intensity provides important advantages for FRET multiplexing. FRET quenches donor fluorescence, thus affecting donor fluorescence lifetime. Unlike intensity measurements, the donor lifetime is insensitive to sources of artefacts such as uneven illumination, subcellular variation in probe concentration, or cell geometry (reviewed in REFS 33–35 and elsewhere). Fluorescence lifetime imaging microscopy (FLIM) expands the number of usable FRET pairs for multiplexing because only the effects on donor fluorescence are measured. Thus, the same acceptor can be used for two different donors[36], and the choice of available proteins can be extended to include non-fluorescent acceptors, such as different versions of dark YFP[37,38]. With current technology, FLIM does incur reduced temporal or spatial resolution relative to wide-field imaging, and not all donor fluorophores are useful for FLIM imaging. However, donor fluorophores and fluorophore combinations with potential for FLIM multiplexing have been described[39–43]: mRFP and GFP, mStrawberry and GFP, mRFP and Venus, mStrawberry and Venus, and mDarkVenus and mGFP were all found to be comparable for FLIM imaging of CaMKII using variants of the Camui sensor, a FRET-based sensor of CaMKII activity.

On the horizon. FRET can also be accomplished using organic dyes, quantum dots and other inorganic fluorophores. Compared with fluorescent proteins, these fluorescent markers provide superior brightness and photostability[44,45], but they are not genetically encoded. Brightness and photostability are important for multiplexing, as they determine how much biosensor must be used in a cell to generate a robust signal. This is especially important when multiple biosensors are loaded in the same cell, as harbouring more biosensors increases cellular perturbation. In a recent study, a FRET biosensor for RHOA was combined with a CDC42 biosensor based on an environment-sensing dye. The dye was attached to a protein domain that bound selectively to activated CDC42 (REF. 22).

On binding activated CDC42, the dye on the biosensor underwent a shift in fluorescence, revealing the localization of CDC42 activity. This design substantially reduced cell perturbation, as it enabled the sensing of endogenous CDC42 and used direct excitation of a bright dye. However, despite their greater sensitivity and ability to operate at lower intracellular concentrations, non-genetic biosensors are rarely used because they have to be loaded into cells via cumbersome methods such as microinjection or electroporation. Recent approaches to attach dyes to proteins *in vivo* show promise for harnessing the advantages of non-genetic fluorophores[46].

Signalling behaviours have also been reported by using only a single fluorescent protein, rather than by FRET. This facilitates experimental multiplexing, as each biosensor uses a smaller portion of the wavelength spectrum. This approach can use different types of biosensor, including fluorescent proteins that respond to ions, pH, voltage or reactive oxygen species[18]. In bimolecular fluorescence complementation (BiFC), a fluorescent protein is split into two non-fluorescent halves, each of which is linked to a different signalling protein. When the two signalling proteins bind, they bring the two halves of the fluorescent protein

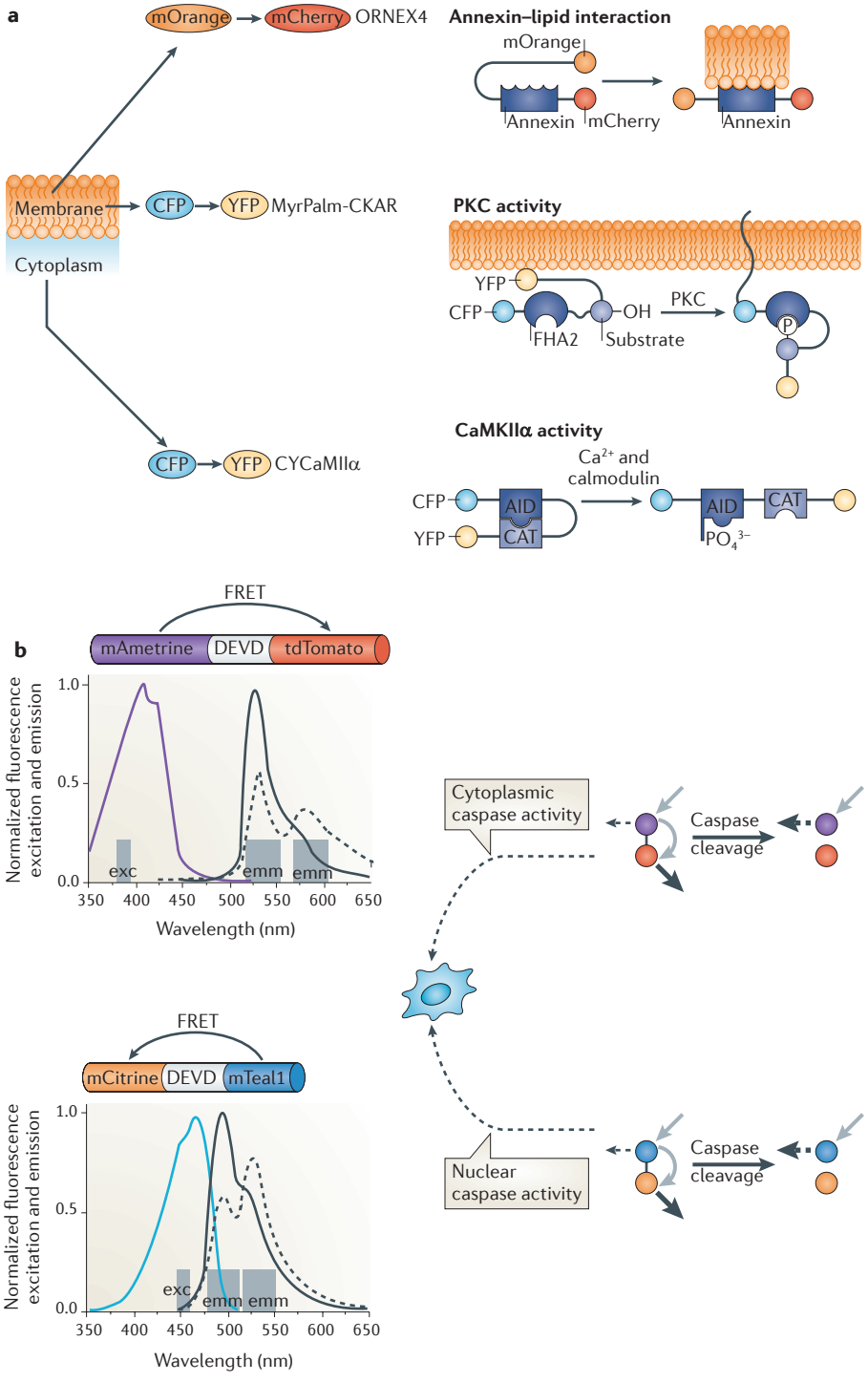

Figure 1 | **Examples of experimental multiplexing. a** | Piljic and Schultz[28] were able to discriminate signals from three biosensors by using both orthogonal fluorescence resonance energy transfer (FRET) pairs and biosensors targeted to different subcellular localizations. They examined the kinetics of protein kinase C (PKC) activity using the MyrPalm-CKAR (C kinase activity reporter)biosensor, the activity of calcium- and calmodulin-dependent kinase IIα (CaMKIIα) using the CYCaMIIα (enhanced yellow fluorescent protein (EYFP)–CaMKIIα–enhanced cyan fluorescent protein (ECFP)) biosensor, and lipid modification using the biosensor ORNEX4 (orange- and red-labelled annexin A4). The monomeric Orange (mOrange) to mCherry FRET of ORNEX4 is abrogated when its annexin component binds to lipid membranes and self-associates. The other two biosensors are based on CFP to YFP FRET. In MyrPalm-CKAR, which is restricted to the plasma membrane, a forkhead-associated 2 (FHA2) domain from the yeast checkpoint protein Rad53 binds to a PKC substrate peptide when the peptide is phosphorylated by PKC[78]. The biosensor CYCaMIIα, restricted to the cytosol, is based on a CYCaMIIα molecule with FRET fluorophores on its termini. Phosphorylation of the autoinhibitory domain (AID) releases the AID from the catalytic domain (CAT), leading to altered FRET[79]. **b** | Ai *et al.*[29] developed a novel fluorescent protein, mAmetrine, which has an unusually large Stokes shift. This facilitated the separation of wavelengths to image two biosensors independently in the same cell, and allowed the simultaneous monitoring of both nuclear and cytoplasmic caspase 3 activity. The Stokes shift enabled fluorophore excitation (exc) and monitoring of emission (emm) at the orthogonal wavelength bands shown by the grey bars. For each FRET pair, a single excitation band is used, leading to emission that is due to either direct excitation of the donor (mAmetrine or mTeal) or FRET emission from the acceptor (tandem dimeric Tomato (tdTomato) or mCitrine). Excitation and emission spectra are shown for the FRET pair in each biosensor, with the colour of the excitation spectra corresponding to the donor fluorophores in the biosensors. In the schematic, grey arrows show the excitation and FRET of the donor fluorophore, whereas black arrows show the level of emission from the donors and acceptors before and after cleavage by caspase 3 at the Asp-Glu-Val-Asp (DEVD) motif that links the FRET pair. Dashed arrows indicate the level of emission from the acceptors before and after cleavage.

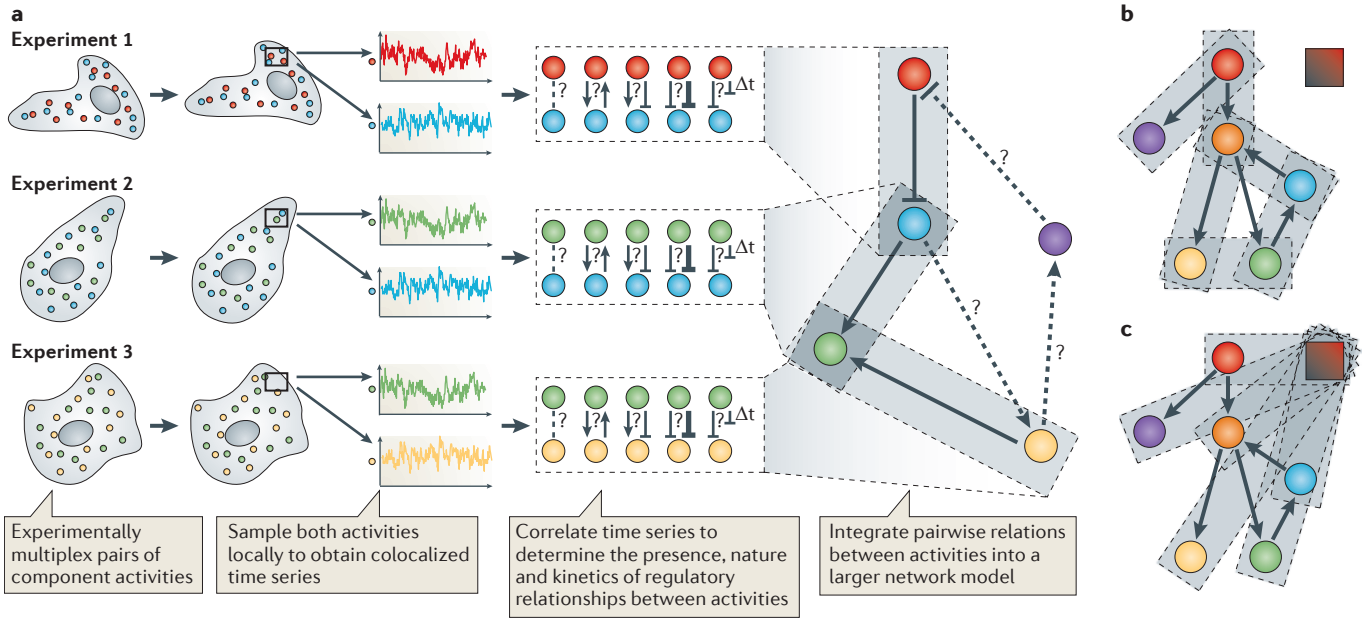

Figure 2 | **Workflow of computational multiplexing. a** | In each of the experiments in a computational multiplexing procedure, a subset of the signalling network components (nodes) are experimentally multiplexed (two are illustrated here). Component activities are sampled locally to extract a colocalized time series for each experimentally multiplexed node, in each subregion of the cell. The sampling windows are defined in a cell-centred frame of reference (see FIG. 4) in order to generate time series that are independent of the cell–cell variation in shape and morphology. These time series are then analysed by correlation methods, testing first the presence of an interaction between the activities (a dashed line means no interaction) and then determining the direction and sign (that is, whether it is stimulatory or inhibitory, see arrows), as well as the timing (by measuring the delay, Δt, between activities), of the interaction. This process is repeated for other activity pairs in the network, with each subsequent experiment sharing a common node with any of the previous experiments. In this illustration, experiments 1 and 2 share observations from the blue node, whereas experiments 2 and 3 share observations from the green node. Continuing this process allows traversal of the network, without requiring each node to be observed simultaneously. Mathematical tools allow the integration of the pairwise, and possibly redundant, observations into a larger network model. In the larger network model, dashed connecting lines indicate possible relationships between activities that can be predicted by the network reconstructions, although no direct observation of these together is available in the raw data. **b**,**c** | Two strategies for traversing the network. In one strategy, the experiment establishes pairwise relationships between activities throughout the network (**b**). In a second strategy, each experiment establishes the relationship of one activity relative to a common fiduciary activity, which is depicted by the red box (**c**).

together, generating fluorescence. In some applications, one half of the fluorescent protein can combine with one of two different second halves[47–51], each generating a unique colour, including a far-red version of the split protein mLumin[52]. This technique is very sensitive because the signal is created over a 'dark' background. However, the interaction of the two halves is currently irreversible and the fluorescence forms with relatively slow kinetics. FRET between identical fluorophores, observed through effects on fluorescence polarization anisotropy (so-called HOMO FRET), has been used to study receptor oligomerization and protein aggregation without the need for two different fluorophores[53–55].

Important strides in experimental multiplexing will have to come from improved sensitivity in biosensor imaging, as toxicity and cell perturbation are important issues when studying low-abundance signalling proteins. Several papers have addressed how the relative concentrations of biosensors and endogenous proteins or molecules affect cell behaviour[56–62]; some others have proposed that sensors can be applied to specific, well-selected proteins, ideally proteins of high concentration that are less likely to be perturbed by introducing biosensors, to reveal the behaviour of larger networks[63,64].

Computational multiplexing

Progress in biosensor design and the spectral decomposition of images, and improvements in filters and instrumentation, will steadily increase the number of simultaneously observable molecular activities. However, deriving a complete analysis of pathway states by studying all of the components in the same cell is unlikely to be possible in the foreseeable future. Thus, methods are needed that complement the direct imaging of multiplexed biosensors with the ability to integrate data from independent experiments into a comprehensive pathway model. These methods are collectively referred to as computational multiplexing (FIG. 2).

Several challenges must be overcome when implementing computational multiplexing approaches. First, the integration of data from multiple experiments implies that the properties of the studied pathway (that is, the hierarchy of pathway components and the kinetics of information transfer between them) do not change between experiments. Practically, this means that the cell state and the environmental conditions are held identical between experiments, for example, by using clonal cell populations. Second, even then, the activation dynamics of the pathway will vary from cell to cell. Therefore, methods for data integration are required that identify, from variable cell responses, a canonical, cell-invariant representation of the pathway. Third, the spatiotemporal coupling of biosensor activities, whether observed in the same or separate experiments, usually results from nonlinear pathways, the feedback and feed-forward relationships of which are unknown a priori. Therefore, data integration must be combined with mathematical approaches for

network inference. In this section, we discuss strategies towards fulfilling these requirements, with reference to studies in which the computational multiplexing of biosensors has provided insights into signalling pathways with subcellular resolution.

A need for conserved experimental conditions. The conservation of the fundamental pathway properties is an implicit assumption made by every investigator who repeats an experiment to average the responses of multiple cells. This is no different with computational multiplexing. However, when combining data from experiments probing different aspects of a pathway with different biosensors, this assumption must be thoroughly validated. The expression or microinjection of a biosensor can shift the pathway properties. To control for such effects, the reproducibility of a cell function related to the studied pathway must be tested for each biosensor that is expressed, over a range of concentrations. For example, for pathways that regulate cell morphogenesis, cell morphology or morphodynamics are excellent measures against which to identify probe-induced biases. These measurements can be accomplished either by manual inspection or, ideally, by quantitative morphological[65] or morphodynamic[66] analyses.

A common fiduciary mark between experiments. To determine the spatiotemporal relationships between activities monitored in independent experiments, spatial and temporal fiduciaries are required that are common between experiments and invariant to changes in cell morphology and cell behaviour. Temporal fiduciaries can be defined by the acute stimulation or inhibition of a pathway[67]. By applying the same intervention protocol across multiple experiments, different biosensor activities can be aligned in time to deduce a response hierarchy. Similarly, spatiotemporal fiduciaries can be defined by spatially limiting the acute stimulation or inhibition of a pathway. Numerous approaches have been proposed to achieve this while monitoring downstream signalling responses, including mechanical stimulation of cells by microspheres[68,69] or photoswitchable reagents[70,71].

Recently, two studies independently established the concept of inferring a response hierarchy from constitutive fluctuations in the activity of biosensors. Time differences between signalling events were determined by temporal and spatial cross-correlation between the activation of two different biosensors and/or between the activation of one biosensor and spontaneous fluctuations in cell morphology[22,24] (FIG. 3). There are several key advantages to this strategy as compared to the acute stimulation or inhibition of a pathway. First, acute interventions may over stimulate or over perturb pathways. As a result, the kinetics and response hierarchies deduced from these experiments may reflect a pathway that operates far outside the range of normal physiology. As well as avoiding this problem, the second advantage of analysing constitutive fluctuations is that this permits dense mapping of spatial gradients in signalling hierarchies. For example, the study of the

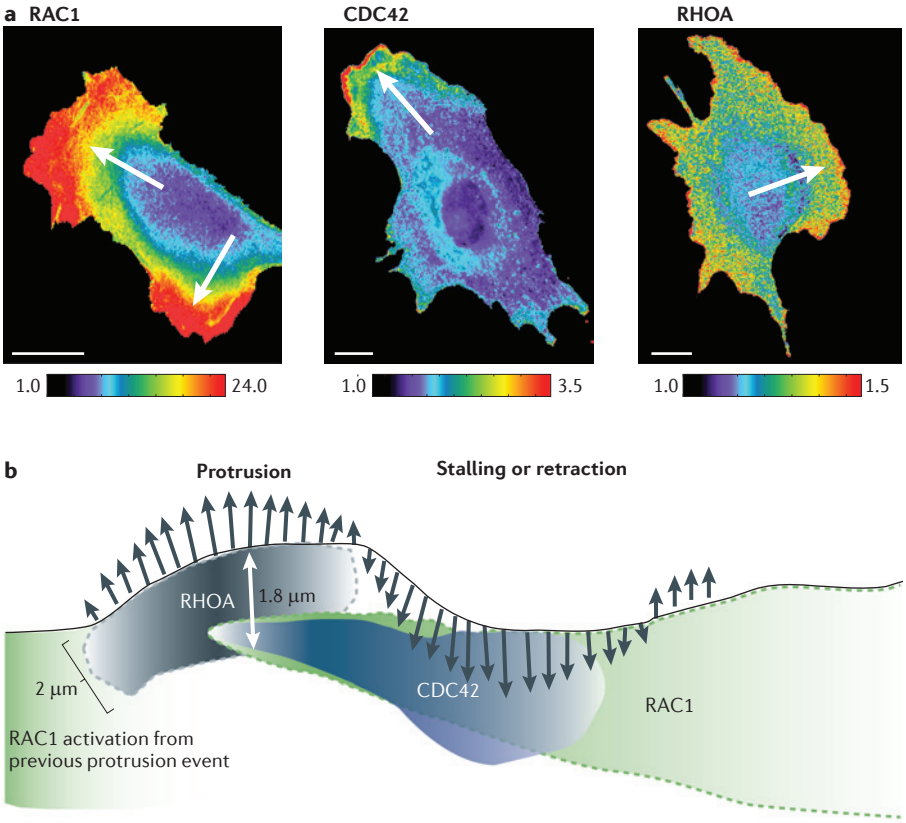

Figure 3 | **Assessing the activity of RHO GTPases using computational multiplexing. a** | Three distinct members of the RHO GTPase family (RAC1, CDC42 and RHOA) were imaged in different cells using different biosensors. To monitor RAC1 activation, a bimolecular fluorescence resonance energy transfer (FRET) reporter was used, which produces a high signal when a RAC-binding fragment of the RAC1 effector p21-activated kinase (PAK), conjugated to cyan fluorescent protein for energy transfer (CyPet), associates with the activated form of RAC1 that is conjugated to yellow fluorescent protein for energy transfer (YPet). To monitor CDC42 activation, an environmentally sensitive dye, mero87, was coupled to a CDC42-binding fragment of the CDC42 effector Wiskott–Aldrich syndrome protein (WASP). Upon association of this labelled fragment with the activated form of CDC42, the dye undergoes a change in its fluorescence spectrum that is observed as a strong increase in fluorescence at a particular wavelength. To monitor RHOA activation, an intramolecular FRET reporter was used. In contrast to the RAC1 reporter, here RHOA and the RHOA-binding fragment are in a single chain, which undergoes conformational changes upon RHOA activation. These changes are detected by changes in the FRET between the CyPet and YPet pair that is part of the single chain sensor. Pseudo-colour scales indicate the dynamic range of the biosensor responses, where 1.0 indicates the minimal response, and the maximum value indicates the strongest response, throughout the time-lapse sequence. Arrows indicate the direction of cell protrusion. **b** | Cartoon illustrating the spatially and temporally differentiated activation of the three RHO GTPases during protrusion (grey arrows pointing up) and retraction or stalling (grey arrows pointing down) events at the cell edge. The shading in the activation 'clouds' get lighter to indicate how the signalling strength decreases over time after initial induction. The relationships between the signalling activities were predicted first indirectly by spatiotemporal cross-correlation analysis of each biosensor, in separate cells, to the velocity of edge movement as a common fiduciary (an example of the strategy described in FIG. 2c). The inferred relationships were then confirmed by direct observation of two of the biosensors (CDC42 and RHOA) in the same cell (an example of the strategy described in FIG. 2b). Figure is reproduced, with permission, from REF. 22

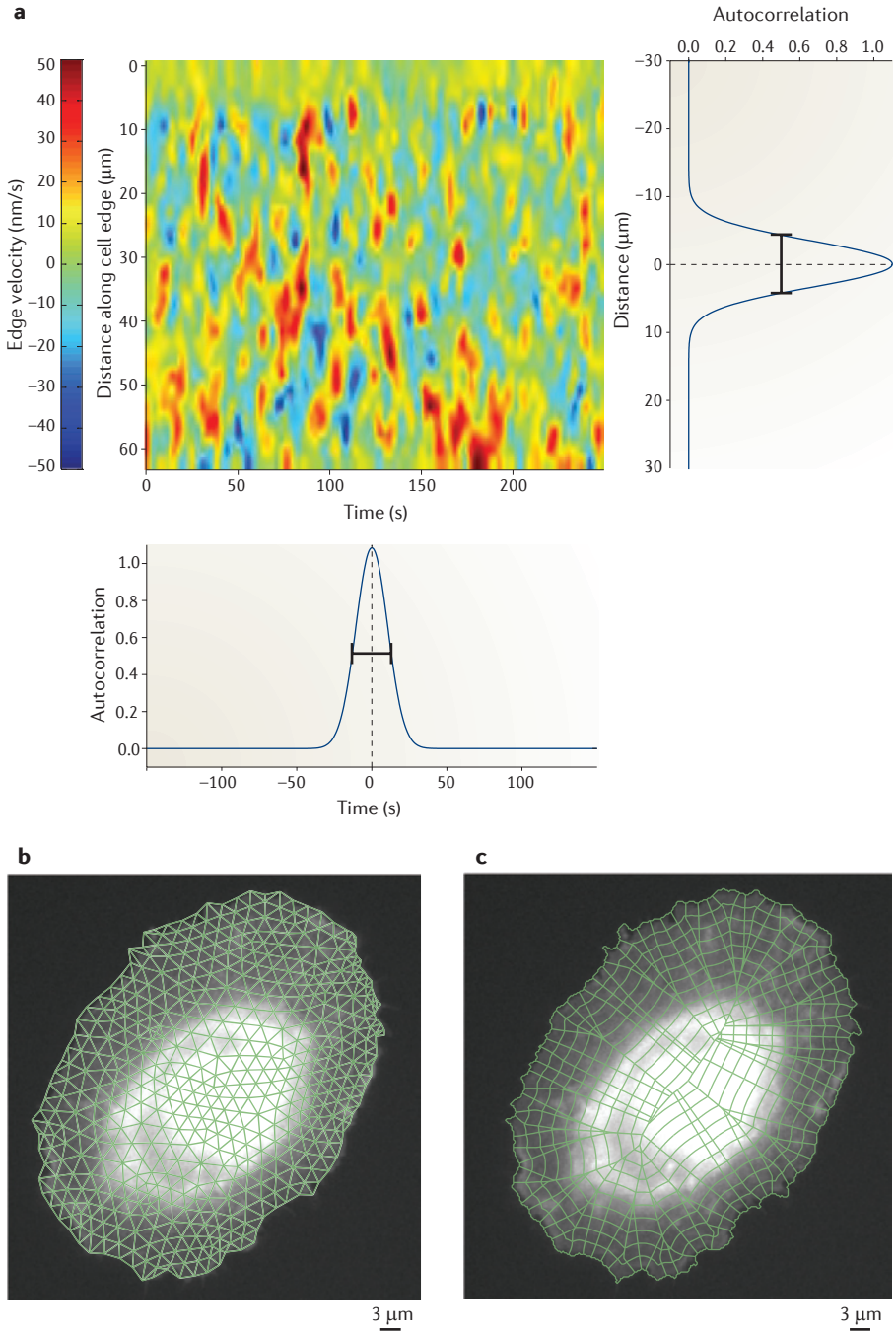

Figure 4 | **Determining the requirements for spatiotemporal sampling to allow computational multiplexing based on constitutive fluctuations. a** | Map of the spatial (vertical axis) and temporal (horizontal axis) activity of an experimental fiduciary (here, cell edge velocity). The activity map displays typical stochastic oscillations, as seen for many cellular activities. The horizontal autocorrelation of the map indicates the characteristic timescale of the oscillations (~40 s in this example, as deduced from the full width at half maximum (FWHM) of the function, black bar). This timescale defines the requirement for temporal sampling. The vertical autocorrelation of the map indicates the characteristic length scale of the oscillations (~15 μm in this example, as deduced from the FWHM, black bar). This length scale defines the requirement for spatial sampling. For both the time and space domains, twofold to fourfold oversampling should be achieved. That is, movies should be acquired at 10 s frame intervals or faster and biosensor intensities should be sampled in probing windows of a maximum of 4 μm side length. **b** | Definition of a triangular mesh of appropriately sized probing windows. **c** | Definition of a polygonal mesh of appropriately sized probing windows. In contrast to the triangular mesh in part **b**, for the polygonal mesh, each window that is inside the cell perimeter has a unique relationship to a window at the cell periphery. Thus, this mode of windowing is preferred for studies that relate intracellular signals to cell protrusion and retraction events.

coordination of RHO GTPases during cell protrusion[22] suggested that the activation of RAC1 is not only delayed by ~40 s, relative to the activation of RHOA, but also is shifted in space by ~2 μm. RHOA is activated at the cell edge, whereas RAC1 is activated behind the cell edge, possibly in growing nascent adhesions. It would be very tedious to derive such predictions of the spatiotemporal organization of pathways from a few scarcely distributed interventions. Third, in concept, fluctuation analysis is readily scalable to pathways involving a very large number of components. To make use of this potential, pairwise cross-correlation analysis must be replaced by more sophisticated mathematical tools that integrate, from multiple experiments, the image fluctuation sequences of partially overlapping sets of component activities.

Appropriate spatiotemporal sampling. The possibility of exploiting constitutive fluctuations to infer the response hierarchy and kinetics of pathways relies on the proper sampling of biosensor activities. The sampling resolution in time must be a few times faster than the shortest timescale of information transmission through the pathway. Otherwise, the fluctuation sequences of different pathway components are decoupled. The sampling resolution in space must be high enough to preclude the averaging of adjacent yet independent pathway events. However, some averaging may be desirable to reduce measurement noise in the fluctuations. As illustrated in FIG. 4, the required time and length scales for sampling signalling activities can be deduced from the autocorrelation functions of the cellular outputs of the pathway; that is, in the example shown, cell protrusion dynamics.

Reconstructing the pathway hierarchy. Until recently, studies involving multiple biosensor activities have used pairwise cross-correlation to infer the relationships between pathway components[22,72]. Component pairs for which the correlation does not reach a defined significance level are considered to be disconnected in the pathway, whereas pairs with a significant correlation are considered to be directly or indirectly coupled. These pairwise analysis methods, although simple, have major limitations. First, as mentioned above, they do not provide the means for a rigorous integration of multiple experiments in one model. Second, cross-correlation approaches break down in the presence of strong feedback and/or feedforward interactions between pathway

Glossary

Fluorescence polarization anisotropy
A technique that measures the rotational diffusion of fluorophores by measuring the difference in the polarization of excitation and emission light. Changes in fluorescence polarization anisotropy indicate changes in the rotational diffusion of molecules that are induced by their interactions with other molecules.

Orthogonal wavelengths
Biosensor emission or excitation wavelengths that are sufficiently different to allow two fluorescent probes to be imaged separately in the same cell.

Pairwise cross-correlation analysis
A technique that uses a mathematical framework to define whether the variation of one time-resolved image activity is coupled or independent of the variation of another time-resolved image activity.

Quantum dots
Small semiconductor crystals that emit light of a longer wavelength on excitation with a shorter wavelength, akin to fluorophores.

Ratiometric imaging
An imaging technique in which biosensors are designed so that the ratio of emission or excitation at two different wavelengths reflects the biological activity being measured. This ratio is independent of the biosensor's fluorescence intensity, so eliminates the effects of cell thickness, uneven biosensor distribution, uneven illumination and other factors.

Spectral decomposition
A mathematical technique to separate the contribution of multiple fluorophore species to the image signal at a certain wavelength. This allows the separation of the signals of fluorophores with overlapping emission spectra.

Stokes shift
The difference between the excitation and emission wavelengths of a fluorescent probe.

components. Third, although temporal cross-correlation generates some evidence for the hierarchy of activation by determining what comes first and what comes second, it cannot define causal relationships between pathway components. Two unconnected activities may be correlated with each other simply because they are downstream of the same activity[73]. Much work is underway to identify causal networks from common fluctuations in gene expression profiles or proteomic data[7,74,75]. Some of these frameworks have even been expanded to non-simultaneously observed data[76]. In contrast to genomic and proteomic data sets, however, biosensor images offer more-finely resolved data about the dynamics and subcellular localization of pathway activities. Although this additional information will greatly enhance the inference of the pathway hierarchy, including the reconstruction of directed interactions between nodes in loops[73], there are significant mathematical challenges in the design of algorithms that integrate data from a sequence of different experiments. A second limitation of these network reconstructions is the type of causality that can be inferred from the graph of directed interactions. Biosensor image analyses alone will predict only a functional causality between network nodes (that is, how information flows between activities). Establishing a molecular causality (that is, how information flows between two nodes because of a particular cascade of molecular interactions) will require complementation of fluctuation analyses by more traditional perturbation approaches. However, because of the exquisite sensitivity and high specificity of biosensor-derived data, subtle molecular perturbations with less risk of uncontrolled side-effects will suffice to identify the mechanisms underlying a particular predicted functional causality.

> "As computational multiplexing provides us with an ability to relate to one another an essentially unlimited number of signalling molecules, biosensor production will become a bottleneck."

Conclusion

In summary, new biosensor designs with extended spectral properties and vastly increased sensitivity have opened exciting opportunities for signal transduction research. It has become possible to simultaneously monitor two or three signalling activities, and enhanced sensitivity permits the analysis of highly localized constitutive pathway fluctuations. This in turn enables the use of powerful statistical formalisms for the integration of multiple experiments and for the inference of hierarchy in signalling networks. Conceptually, this has brought us to the point at which complex pathways, with many components and redundant and nonlinear cascades, can be studied in living cells under nearly physiological conditions. However, developments on the horizon will play a major part in turning this concept into a routine tool for the cell biologist. To apply computational multiplexing by relying on combinations of biosensors in the same cell, issues of cell perturbation will become even more important in biosensor design.

To overcome these issues, biosensors must be developed that have enhanced sensitivity, which would enable their effective use at lower concentrations; this sensitivity may stem from the use of brighter fluorophores, direct excitation or improvements in instrumentation. Designs responding to endogenous proteins will also reduce cell perturbation. Novel approaches to decrease the spectral bandwidth of each biosensor will increase the number of activities that can be imaged simultaneously and might include the development of FLIM with an enhanced signal to noise ratio, biosensors that are based on single fluorophores, and spectral deconvolution imaging. As computational multiplexing provides us with an ability to relate to one another an essentially unlimited number of signalling molecules, biosensor production will become a bottleneck. Soon, biosensors will not need to be based on naturally occurring domains or substrates with the desired specificity, but will be generated via the high-throughput screening of engineered scaffolds[77].

Christopher M. Welch and Klaus M. Hahn are at the Department of Pharmacology and Lineberger Cancer Center, University of North Carolina at Chapel Hill, Chapel Hill, North Carolina 27599, USA.

Hunter Elliott and Gaudenz Danuser are at the Department of Cell Biology, Harvard Medical School, Boston, Massachusetts 02115, USA.

C.M.W and H.E contributed equally to this work.

Correspondence to G.D. and K.M.H.
e-mails: Gaudenz_Danuser@hms.harvard.edu; khahn@med.unc.edu

doi:10.1038/nrm3212

1. Olsen, J. V. *et al.* Global, *in vivo*, and site-specific phosphorylation dynamics in signaling networks. *Cell* **127**, 635–648 (2006).
2. Barrios-Rodiles, M. *et al.* High-throughput mapping of a dynamic signaling network in mammalian cells. *Science* **307**, 1621–1625 (2005).
3. Margolin, A. A. *et al.* ARACNE: An algorithm for the reconstruction of gene regulatory networks in a mammalian cellular context. *BMC Bioinformatics* **7** (Suppl. 1), S7 (2006).
4. Spencer, S. L., Gaudet, S., Albeck, J. G., Burke, J. M. & Sorger, P. K. Non-genetic origins of cell-to-cell variability in TRAIL-induced apoptosis. *Nature* **459**, 428–432 (2009).
5. Colman-Lerner, A. *et al.* Regulated cell-to-cell variation in a cell-fate decision system. *Nature* **437**, 699–706 (2005).
6. Cohen-Saidon, C., Cohen, A. A., Sigal, A., Liron, Y. & Alon, U. Dynamics and variability of ERK2 response to EGF in individual living cells. *Mol. Cell* **36**, 885–893 (2009).
7. Sachs, K., Perez, O., Pe'er, D., Lauffenburger, D. A. & Nolan, G. P. Causal protein-signaling networks derived from multiparameter single-cell data. *Science* **308**, 523–529 (2005).
8. Salmon, W. C., Adams, M. C. & Waterman-Storer, C. M. Dual-wavelength fluorescent speckle microscopy reveals coupling of microtubule and actin movements in migrating cells. *J. Cell Biol.* **158**, 31–37 (2002).
9. Schaefer, A. W. *et al.* Coordination of actin filament and microtubule dynamics during neurite outgrowth. *Dev. Cell* **15**, 146–162 (2008).

10. Hu, K., Ji, L., Applegate, K. T., Danuser, G. & Waterman-Storer, C. M. Differential transmission of actin motion within focal adhesions. *Science* **315**, 111–115 (2007).
11. Taylor, M. J., Perrais, D. & Merrifield, C. J. A high precision survey of the molecular dynamics of mammalian clathrin-mediated endocytosis. *PLoS Biol.* **9**, e1000604 (2011).
12. Harbeck, M. C. *et al.* Simultaneous optical measurements of cytosolic Ca^{2+} and cAMP in single cells. *Sci. STKE* **2006**, PL6 (2006).
13. Wier, W. G., Rizzo, M. A., Raina, H. & Zacharia, J. A technique for simultaneous measurement of Ca^{2+}, FRET fluorescence and force in intact mouse small arteries. *J. Physiol.* **586**, 2437–2443 (2008).
14. Tengholm, A., Teruel, M. N. & Meyer, T. Single cell imaging of PI3K activity and glucose transporter insertion into the plasma membrane by dual color evanescent wave microscopy. *Sci. STKE* **2003**, PL4 (2003).
15. Tanimura, A., Nezu, A., Morita, T., Turner, R. J. & Tojyo, Y. Fluorescent biosensor for quantitative real-time measurements of inositol 1,4,5-trisphosphate in single living cells. *J. Biol. Chem.* **279**, 38095–38098 (2004).
16. Kitano, M., Nakaya, M., Nakamura, T., Nagata, S. & Matsuda, M. Imaging of Rab5 activity identifies essential regulators for phagosome maturation. *Nature* **453**, 241–245 (2008).
17. VanEngelenburg, S. B. & Palmer, A. E. Fluorescent biosensors of protein function. *Curr. Opin. Chem. Biol.* **12**, 60–65 (2008).
18. Newman, R. H., Fosbrink, M. D. & Zhang, J. Genetically encodable fluorescent biosensors for tracking signaling dynamics in living cells. *Chem. Rev.* **111**, 3614–3666 (2011).
19. Hoppe, A. D. & Swanson, J. A. Cdc42, Rac1, and Rac2 display distinct patterns of activation during phagocytosis. *Mol. Biol. Cell* **15**, 3509–3519 (2004).
20. Swanson, J. A. & Hoppe, A. D. The coordination of signaling during Fc receptor-mediated phagocytosis. *J. Leukoc. Biol.* **76**, 1093–1103 (2004).
21. Vaughan, E. M., Miller, A. L., Yu, H. Y. & Bement, W. M. Control of local Rho GTPase crosstalk by Abr. *Curr. Biol.* **21**, 270–277 (2011).
22. Machacek, M. *et al.* Coordination of Rho GTPase activities during cell protrusion. *Nature* **461**, 99–103 (2009).
23. Ji, L., Lim, J. & Danuser, G. Fluctuations of intracellular forces during cell protrusion. *Nature Cell Biol.* **10**, 1393–1400 (2008).
24. Tsukada, Y. *et al.* Quantification of local morphodynamics and local GTPase activity by edge evolution tracking. *PLoS Comput. Biol.* **4**, e1000223 (2008).
25. Matz, M. V. *et al.* Fluorescent proteins from nonbioluminescent Anthozoa species. *Nature Biotech.* **17**, 969–973 (1999).
26. Shaner, N. C. *et al.* Improved monomeric red, orange and yellow fluorescent proteins derived from *Discosoma* sp. red fluorescent protein. *Nature Biotech.* **22**, 1567–1572 (2004).
27. Shaner, N. C. *et al.* Improving the photostability of bright monomeric orange and red fluorescent proteins. *Nature Methods* **5**, 545–551 (2008).
28. Piljic, A. & Schultz, C. Simultaneous recording of multiple cellular events by FRET. *ACS Chem. Biol.* **3**, 156–160 (2008).
29. Ai, H. W., Hazelwood, K. L., Davidson, M. W. & Campbell, R. E. Fluorescent protein FRET pairs for ratiometric imaging of dual biosensors. *Nature Methods* **5**, 401–403 (2008).
30. Niino, Y., Hotta, K. & Oka, K. Blue fluorescent cGMP sensor for multiparameter fluorescence imaging. *PLoS ONE* **5**, e9164 (2010).
31. Niino, Y., Hotta, K. & Oka, K. Simultaneous live cell imaging using dual FRET sensors with a single excitation light. *PLoS ONE* **4**, e6036 (2009).
32. Tomosugi, W. *et al.* An ultramarine fluorescent protein with increased photostability and pH insensitivity. *Nature Methods* **6**, 351–353 (2009).
33. Jares-Erijman, E. A. & Jovin, T. M. FRET imaging. *Nature Biotech.* **21**, 1387–1395 (2003).
34. Jares-Erijman, E. A. & Jovin, T. M. Imaging molecular interactions in living cells by FRET microscopy. *Curr. Opin. Chem. Biol.* **10**, 409–416 (2006).
35. Wallrabe, H. & Periasamy, A. Imaging protein molecules using FRET and FLIM microscopy. *Curr. Opin. Biotechnol.* **16**, 19–27 (2005).
36. Peyker, A., Rocks, O. & Bastiaens, P. I. Imaging activation of two Ras isoforms simultaneously in a single cell. *Chembiochem* **6**, 78–85 (2005).
37. Murakoshi, H., Lee, S. J. & Yasuda, R. Highly sensitive and quantitative FRET–FLIM imaging in single dendritic spines using improved non-radiative YFP. *Brain Cell Biol.* **36**, 31–42 (2008).
38. Ganesan, S., Ameer-Beg, S. M., Ng, T. T., Vojnovic, B. & Wouters, F. S. A dark yellow fluorescent protein (YFP)-based resonance energy-accepting chromoprotein (REACh) for Förster resonance energy transfer with GFP. *Proc. Natl Acad. Sci. USA* **103**, 4089–4094 (2006).
39. Kwok, S. *et al.* Genetically encoded probe for fluorescence lifetime imaging of CaMKII activity. *Biochem. Biophys. Res. Commun.* **369**, 519–525 (2008).
40. Kremers, G. J., van Munster, E. B., Goedhart, J. & Gadella, T. W. Jr. Quantitative lifetime unmixing of multiexponentially decaying fluorophores using single-frequency fluorescence lifetime imaging microscopy. *Biophys. J.* **95**, 378–389 (2008).
41. Goedhart, J., Vermeer, J. E., Adjobo-Hermans, M. J., van Weeren, L. & Gadella, T. W. Jr. Sensitive detection of p65 homodimers using red-shifted and fluorescent protein-based FRET couples. *PLoS ONE* **2**, e1011 (2007).
42. Shcherbo, D. *et al.* Practical and reliable FRET/FLIM pair of fluorescent proteins. *BMC Biotechnol.* **9**, 24 (2009).
43. Padilla-Parra, S. *et al.* Quantitative comparison of different fluorescent protein couples for fast FRET-FLIM acquisition. *Biophys. J.* **97**, 2368–2376 (2009).
44. Sapsford, K. E., Berti, L. & Medintz, I. L. Materials for fluorescence resonance energy transfer analysis: beyond traditional donor-acceptor combinations. *Angew. Chem. Int. Ed. Engl.* **45**, 4562–4589 (2006).
45. Pertz, O. & Hahn, K. M. Designing biosensors for Rho family proteins--deciphering the dynamics of Rho family GTPase activation in living cells. *J. Cell Sci.* **117**, 1313–1318 (2004).
46. Hinner, M. J. & Johnsson, K. How to obtain labeled proteins and what to do with them. *Curr. Opin. Biotechnol.* **21**, 766–776 (2010).
47. Hu, C.-D. & Kerppola, T. K. Simultaneous visualization of multiple protein interactions in living cells using multicolor fluorescence complementation analysis. *Nature Biotech.* **21**, 539–545 (2003).
48. Kodama, Y. & Wada, M. Simultaneous visualization of two protein complexes in a single plant cell using multicolor fluorescence complementation analysis. *Plant Mol. Biol.* **70**, 211–217 (2009).
49. Vidi, P. A., Chemel, B. R., Hu, C. D. & Watts, V. J. Ligand-dependent oligomerization of dopamine D_2 and adenosine A_{2A} receptors in living neuronal cells. *Mol. Pharmacol.* **74**, 544–551 (2008).
50. Grinberg, A. V., Hu, C. D. & Kerppola, T. K. Visualization of Myc/Max/Mad family dimers and the competition for dimerization in living cells. *Mol. Cell Biol.* **24**, 4294–4308 (2004).
51. Michnick, S. W., Ear, P. H., Manderson, E. N., Remy, I. & Stefan, E. Universal strategies in research and drug discovery based on protein-fragment complementation assays. *Nature Rev. Drug Discov.* **6**, 569–582 (2007).
52. Chu, J. *et al.* A novel far-red bimolecular fluorescence complementation system that allows for efficient visualization of protein interactions under physiological conditions. *Biosens. Bioelectron.* **25**, 234–239 (2009).
53. Altman, D., Goswami, D., Hasson, T., Spudich, J. A. & Mayor, S. Precise positioning of myosin VI on endocytic vesicles *in vivo*. *PLoS Biol.* **5**, e210 (2007).
54. Sharma, P. *et al.* Nanoscale organization of multiple GPI-anchored proteins in living cell membranes. *Cell* **116**, 577–589 (2004).
55. Varma, R. & Mayor, S. GPI-anchored proteins are organized in submicron domains at the cell surface. *Nature* **394**, 798–801 (1998).
56. Pertz, O., Hodgson, L., Klemke, R. L. & Hahn, K. M. Spatiotemporal dynamics of RhoA activity in migrating cells. *Nature* **440**, 1069–1072 (2006).
57. Nalbant, P., Hodgson, L., Kraynov, V., Toutchkine, A. & Hahn, K. M. Activation of endogenous Cdc42 visualized in living cells. *Science* **305**, 1615–1619 (2004).
58. Kraynov, V. S. *et al.* Localized Rac activation dynamics visualized in living cells. *Science* **290**, 333–337 (2000).
59. Berlin, J. R., Bassani, J. W. & Bers, D. M. Intrinsic cytosolic calcium buffering properties of single rat cardiac myocytes. *Biophys. J.* **67**, 1775–1787 (1994).
60. Helmchen, F., Imoto, K. & Sakmann, B. Ca^{2+} buffering and action potential-evoked Ca^{2+} signaling in dendrites of pyramidal neurons. *Biophys. J.* **70**, 1069–1081 (1996).
61. Mochizuki, N. *et al.* Spatio-temporal images of growth-factor-induced activation of Ras and Rap1. *Nature* **411**, 1065–1068 (2001).
62. Sawano, A., Takayama, S., Matsuda, M. & Miyawaki, A. Lateral propagation of EGF signaling after local stimulation is dependent on receptor density. *Dev. Cell* **3**, 245–257 (2002).
63. Schultz, C., Schleifenbaum, A., Goedhart, J. & Gadella, T. W. Jr. Multiparameter imaging for the analysis of intracellular signaling. *Chembiochem* **6**, 1323–1330 (2005).
64. Miyawaki, A. Visualization of the spatial and temporal dynamics of intracellular signaling. *Dev. Cell* **4**, 295–305 (2003).
65. Bakal, C., Aach, J., Church, G. & Perrimon, N. Quantitative morphological signatures define local signaling networks regulating cell morphology. *Science* **316**, 1753–1756 (2007).
66. Machacek, M. & Danuser, G. Morphodynamic profiling of protrusion phenotypes. *Biophys. J.* **90**, 1439–1452 (2006).
67. Taylor, R. J. *et al.* Dynamic analysis of MAPK signaling using a high-throughput microfluidic single-cell imaging platform. *Proc. Natl Acad. Sci. USA* **106**, 3758–3763 (2009).
68. Kiosses, W. B., Shattil, S. J., Pampori, N. & Schwartz, M. A. Rac recruits high-affinity integrin αvβ3 to lamellipodia in endothelial cell migration. *Nature Cell Biol.* **3**, 316–320 (2001).
69. Wang, Y. *et al.* Visualizing the mechanical activation of Src. *Nature* **434**, 1040–1045 (2005).
70. Levskaya, A., Weiner, O. D., Lim, W. A. & Voigt, C. A. Spatiotemporal control of cell signalling using a light-switchable protein interaction. *Nature* **461**, 997–1001 (2009).
71. Wu, Y. I. *et al.* A genetically encoded photoactivatable Rac controls the motility of living cells. *Nature* **461**, 104–108 (2009).
72. Tkachenko, E. *et al.* Protein kinase a governs a RhoA-RhoGDI-driven protrusion-retraction pacemaker in migrating cells. *Nature Cell Biol.* **13**, 660–667 (2011).
73. Vilela, M. & Danuser, G. What's wrong with correlative experiments? *Nature Cell Biol.* **13**, 1011 (2011).
74. Locasale, J. W. & Wolf-Yadlin, A. Maximum entropy reconstructions of dynamic signaling networks from quantitative proteomics data. *PLoS ONE* **4**, e6522 (2009).
75. Perrin, B. E. *et al.* Gene networks inference using dynamic Bayesian networks. *Bioinformatics* **19** (Suppl. 2), ii138–ii148 (2003).
76. Sachs, K. *et al.* Learning signaling network structures with sparsely distributed data. *J. Comput. Biol.* **16**, 201–212 (2009).
77. Gulyani, A. *et al.* A biosensor generated via high-throughput screening quantifies cell edge Src dynamics. *Nature Chem. Biol.* **7**, 437–444 (2011).
78. Violin, J. D., Zhang, J., Tsien, R. Y. & Newton, A. C. A genetically encoded fluorescent reporter reveals oscillatory phosphorylation by protein kinase C. *J. Cell Biol.* **161**, 899–909 (2003).
79. Takao, K. *et al*. Visualization of synaptic Ca^{2+}/calmodulin-dependent protein kinase II activity in living neurons. *J. Neurosci.* **25**, 3107–3112 (2005).

Acknowledgements
This work was funded by the US National Institutes of Health grants R01 GM90317 (to G.D. and K.H) and GM057464 (to K.H.) and the Cell Migration Consortium (U54 GM64346).

Competing interests statement
The authors declare no competing financial interests.

FURTHER INFORMATION
Gaudenz Danuser's homepage: http://lccb.hms.harvard.edu
Klaus M. Hahn's homepage: http://hahnlab.com

SUPPLEMENTARY INFORMATION
See online article: S1 (figure) | S2 (table)

ALL LINKS ARE ACTIVE IN THE ONLINE PDF